JOURNAL OF
Materials
CHEMISTRY

Characterization of iron-doped titania sol–gel materials

T. López,*[a] J. A. Moreno,[a] R. Gómez,[a] X. Bokhimi,[a] J. A. Wang,[b] H. Yee-Madeira,[b] G. Pecchi[c] and P. Reyes[c]

[a] *Universidad Autónoma Metropolitana-Iztapalapa, Departament of Chemistry, P.O. Box 55-534, México D. F. 09340. E-mail: tesy@xanum.uam.mx*
[b] *Escuela Superior de Ingeniería Química (ESIQIE), IPN, Zacatenco, UPALM, 07738, México D.F.*
[c] *Departament of Physical Chemistry, Faculty of Chemical Science, University of Concepcion, P.O. Box: 160-C, Concepcion, Chile. Tel: 56-41-204324; Fax: 56-41-245974*

Received 29th June 2001, Accepted 6th November 2001
First published as an Advance Article on the web 4th February 2002

Fe/TiO_2 materials at 1 wt% Fe content have been prepared by the addition of aqueous solutions of $FeCl_2$ to titanium *n*-tetrabutoxide using hydrochloric acid (pH 3) as a hydrolysis catalyst. The obtained gel was thermally treated at 200, 400, 600 and 800 °C. Characterization of the materials was performed by FTIR, UV–Vis, Mössbauer and X-ray powder diffraction. FTIR spectra of the calcined samples showed the presence of highly hydroxylated TiO_2. The XRD patterns show the coexistance of brookite, anatase and rutile TiO_2 phases in samples treated up to 600 °C. In the sample treated at 800 °C rutile was the only phase observed. UV–Vis spectroscopy revealed that the band gap E_g of the samples increased with increased thermal treatment temperature. Mössbauer spectroscopy showed the coexistance of Fe^{2+} and Fe^{3+} on the TiO_2 samples treated at high temperatures.

Introduction

The synthesis of metallic oxides by the sol–gel process is presently a widely accepted method for the preparation of such materials, in particular when it is desired to incorporate other metallic ions in the gels.[1–7] Several important features characterize these solids, which make them differ considerably from those prepared by more conventional methods. The high purity of the oxides obtained by the sol–gel method and the relatively much lower temperatures necessary for their synthesis, are among the most noticeable aspects from the points of view of quality and economy.[8]

The final properties shown by these materials depend on the hydrolysis catalyst, the pH of the gelling solution, the nature of the impurities added before gelling,[8,9] and the thermal treatment. All these factors play an important role in the synthesis of metallic oxides, especially when the oxides form well-defined crystalline structures. That is so for TiO_2 in which the relative abundance of rutile or anatase phases strongly depends on the synthesis conditions and thermal treatments applied during the gel evolution.[9–11]

When titania is prepared by the sol method, it can be obtained with a crystallite size in the range of nanometers.[12] The chemical, electrical and catalytic properties of titania can be modified by the incorporation of metallic ions. Metal doping could induce the formation of oxygen vacancies in the structure as well as stabilization of titanium in the unusual Ti^{3+} oxidation state.[13–18] The preparation of TiO_2 with crystallite sizes in the nanometer range also induces the formation of non-stoichiometric Ti : O ratios in the rutile or anatase phases.[19]

In most instances nanocrystalline structures are obtained when the sol–gel method is used to synthesize titania.[20–22] It has been reported that the starting gels are not completely hydrolyzed and such behavior could be responsible for the formation of very small nanocrystallites. The initial gels can be described by the following formula:

$$Ti_nO_{2n-(x+y)/2}(OH)_x(OR)_y$$

where *n*, *x* and *y* are the number of titanium atoms, terminal OH and OR groups, respectively.[18]

The doping of titania gels with iron(II) ions using an aqueous solution containing $FeCl_2$ and hydrochloric acid as doping solution could produce materials showing interesting magnetic properties. The chemistry of $FeCl_2$ is well described by Cotton and Wilkinson.[23] The addition of hydrochloric acid to $FeCl_2$ in aqueous solution leads to the hexahydrate iron(II) halide $[FeCl_2{\cdot}6H_2O]$ and octahedral *trans*-$[FeCl_2(H_2O)_4]$, while the direct reaction with chlorine gives the iron(III) halide. In iron(II) aqueous solutions containing no complexing agents, the hexaquo iron(II) ion $[Fe(H_2O)_6]$ is present. Since the redox potential in acid solution for the couple Fe^{3+}–Fe^{2+} is 0.771 V, it is possible for molecular oxygen to oxidize Fe^{2+} to Fe^{3+} [eqn. (1)].

$$2\,Fe^{2+} + \tfrac{1}{2}\,O_2 + 2H^+ \rightarrow 2\,Fe^{3+} + H_2O,\ E^0 = 0.46\ \mathrm{V} \quad (1)$$

The oxidation of Fe^{2+} to Fe^{3+} by molecular oxygen is likely to proceed *via* the formation of FeO_2^{2+}, in which the oxygen may be bound as in the iridium complex $O_2Ir(PPh_3)_2(CO)Cl$.[24]

Iron(II) species can be stabilized in sol–gel systems, since the hydroxy groups present in the titania are important reducing agents [eqn. (2)].

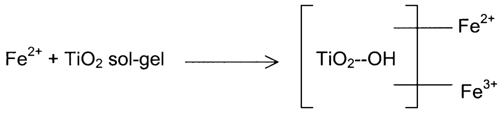

(2)

To prevent oxidation of Fe^{2+} ions during the gelling of titanium alkoxide using hydrochloric acid as hydrolysis

DOI: 10.1039/b105724n

catalyst, it is necessary to extend the alkoxide hydrolysis rate. Thus is possible if the gelling of the alkoxides is performed under acidic conditions.[25]

The present work reports the synthesis of sol–gel Fe/TiO_2 materials prepared under acidic (pH 3) hydrolysis conditions using titanium alkoxide and $FeCl_2$ in HCl media as initial precursors. Samples calcined at 200, 400, 600 and 800 °C were characterized by FTIR, UV–Vis and Mössbauer spectroscopy and X-ray powder diffraction.

Experimental

Sample preparation. Fe/TiO_2-pH 3-1% materials containing 1.0 wt% iron were prepared as follows: to a solution containing 15.0 ml of bi-distilled water and 50.0 ml of ethanol were added 0.045 g of $FeCl_2{\cdot}2H_2O$ (Baker 99.9%) and 0.4 ml of HCl (Baker, 35% v/v), to adjust the solution to pH 3. The solution was allowed to reflux at 70 °C with constant stirring and then 84.5 ml of $Ti(n\text{-}OBu)_4$ (Strem Chemicals 98%) was added dropwise to the solution. The resulting sol was maintained at 70 °C under reflux for 24 hours until a gel was formed.

The gels were dried and then calcined at 200, 400, 600 or 800 °C for 4 h at a heating rate of 3 °C min^{-1}.

Specific surface areas. The specific surface areas of the calcined solids were evaluated from N_2 isotherms obtained with an ASAP2000 Micromeritics apparatus. The BET and BJH methods were used to calculate the specific areas and the mean pore size diameter, respectively.

FTIR. Fourier transform infrared spectra in the wavenumber region 4000–400 cm^{-1} were obtained on a Perkin Elmer 1600 spectrometer. Pre-treated powders were pressed until transparent clear pellets were obtained for measurement.

UV–Vis. Diffuse reflectance spectra were obtained with a Varian Cary III spectrometer. The Fe/TiO_2 powders were placed in a quartz cell for measurement in the range 200–800 nm. The reference used was MgO (100% reflectance).

XRD. XRD studies of the Fe/TiO_2 materials were performed in a Siemens D-500 difractometer coupled to a Cu X-ray tube, the Cu-Kα wavelength of which was selected by means of a nickel filter.

Mössbauer technique. Mössbauer spectra were obtained with a Wissel apparatus using ^{57}Co in iron foil as the radiation source.

Results and discussion

Specific surface areas. The BET specific surface areas as well as the mean pore diameter of the samples are reported in Table 1. It can be seen that thermal treatment leads to strong diminution of the specific surface areas which diminish from 200 to 3.0 $m^2\ g^{-1}$, while the mean pore diameter increases from 4.6 to 22.7 nm in samples treated at 200 and 800 °C, respectively. This behavior is typical for thermally treated metal oxides.

Table 1 Forbidden band gap, E_g, specific surface areas and mean pore diameter for Fe/TiO_2 (1% wt) materials treated at various temperatures

Material	E_g/eV	Surface area/$m^2\ g^{-1}$	Mean pore diameter/nm
Fe/TiO_2 pH 3-200 °C	2.2	200	4.6
Fe/TiO_2 pH 3-400 °C	2.4	95	9.2
Fe/TiO_2 pH 3-600 °C	2.6	40	12.3
Fe/TiO_2 pH 3-800 °C	3.0	3	22.7

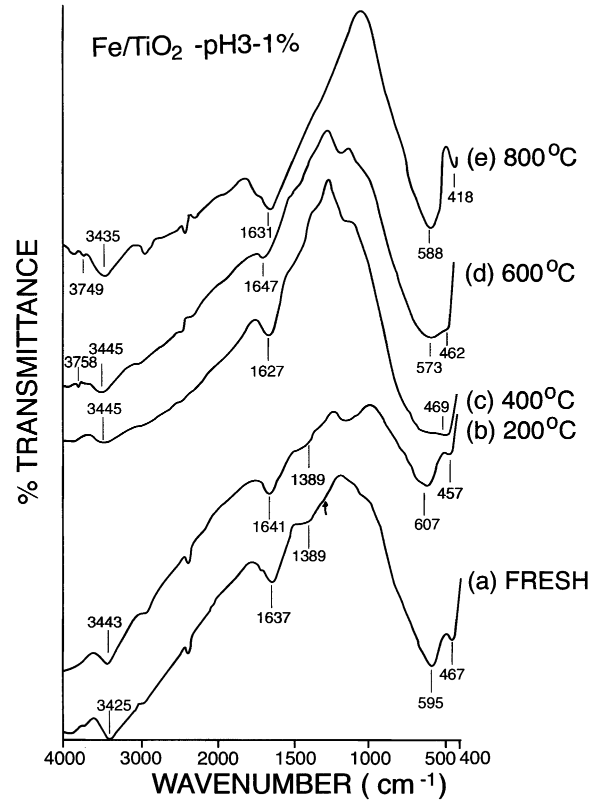

Fig. 1 FTIR spectra of Fe/TiO_2 pH 3 materials treated at various temperatures: (a) 70 °C, (b) 200 °C, (c) 400 °C, (d) 600 °C and (e) 800 °C.

FTIR. Fig. 1 shows FTIR spectra of the thermally treated samples. Fig. 1(a) shows the spectrum of a fresh Fe/TiO_2 sample dried at 70 °C. A broad peak can be seen at 3425 cm^{-1}, assigned to stretching vibration mode of the OH groups within the TiO_2 sol–gel.[24] The corresponding bending vibration band can be observed at 1637 cm^{-1}. The TiO_2–OH bonds arise from the hydrolysis reactions occurring during the gelling of the titanium alkoxide as shown below.[26,27]

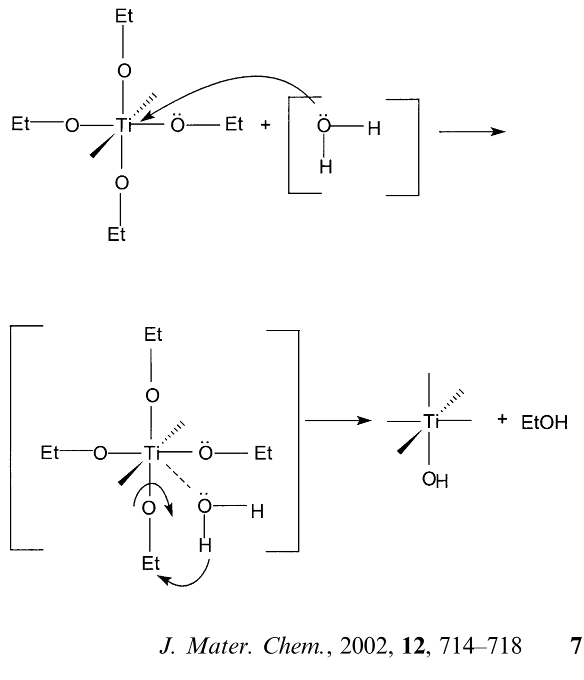

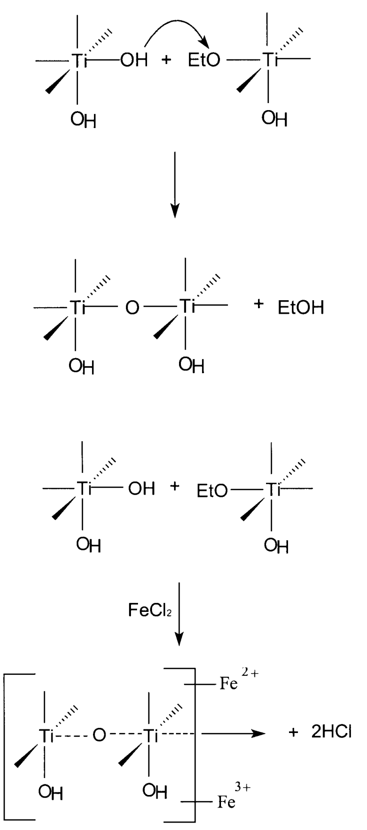

An additional band observed at 1389 cm^{-1} is assigned to asymmetric bending vibrations of C–H bonds.[28] In the low energy region of the spectrum the bands at 595 and 467 cm^{-1} are assigned to bending vibrations of Ti–O bonds.

When the temperature is raised to 200 °C (Fig. 1(b)), the intensity of the OH vibration bands is maintained and the Ti–O bending vibration bands are shifted towards higher energy due to structural rearrangements. In the sample treated at 400 °C (Fig. 1(c)) the 1389 cm^{-1} band disappears due to the total desorption of organic residual groups and in the low energy region of the spectrum the two bands at 607 and 457 cm^{-1} observed in the sample treated at 200 °C are now unresolved.

After heating the sample at 600 °C (Fig. 1(d)), the intensity of the bending OH vibration decreases and the low energy region was totally undefined. The FTIR spectrum of the sample treated at 800 °C (Fig. 1(e)) is practically the same as that observed for the 600 °C treated sample. It should be noted that even when the sample was treated at 800 °C, the OH vibration can be observed. Thus the sample maintains a certain degree of hydroxylation.

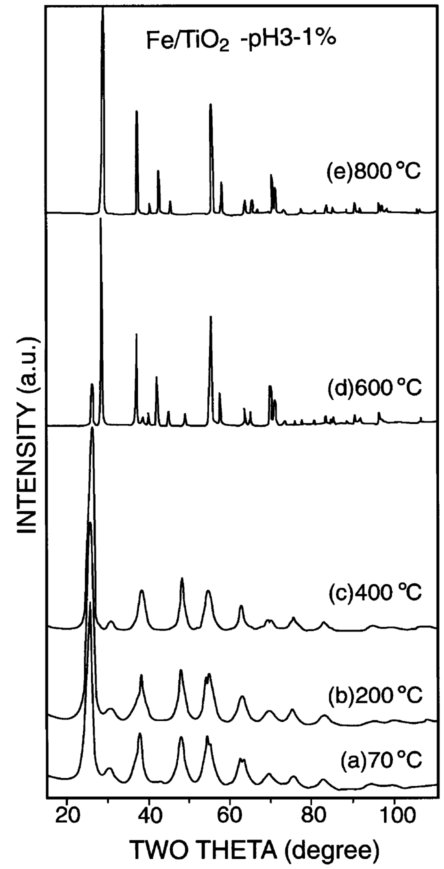

Fig. 2 X-Ray diffractogram of Fe/TiO_2 pH 3 samples treated at various temperatures: (a) 70 °C, (b) 200 °C, (c) 400 °C, (d) 600 °C and (e) 800 °C.

XRD spectra

XRD patterns of the samples heated at various temperatures are shown in Fig. 2. The samples treated at 70, 200 and 400 °C (Fig. 2(a), (b) and (c)) show a mixture of the brookite, anatase and rutile phases of titania, the highest intensity peak corresponding to the (101) planes of the anatase crystalline form of TiO_2 at $2\theta = 25.2°$, giving an interplanar distance $d = 1.81$ Å.[29] For the sample treated at 600 °C, the intensity of the anatase peak decreases while the rutile peak increases and the brookite phase disappears (Fig. 2(d)). In this sample the peak corresponding to the rutile phase is that of highest intensity. In the sample treated at 800 °C the anatase form completely disappears and rutile is the only phase that can be observed. The transformation in the order brookite, anatase, rutile is that expected during the stabilization of titania gels. It can be considered that the iron does not have a significant effect on the stabilization of the different titania phases.

UV–Vis (diffuse reflectance) spectroscopy

UV–Vis diffuse reflectance spectra of the Fe/TiO_2 samples are shown in Fig. 3. From these spectra, the E_g values of the samples were calculated using eqn. (3):

$$\alpha(h\nu) = A(h\nu - E_g)^{m/2} \qquad (3)$$

where α is the absorption coefficient, $h\nu$ is the photon energy, $m = 1$ for direct transition between bands and E_g is the energy of the band gap. For practical purposes E_g was calculated by extrapolation of the absorption band to the x-axis. The values

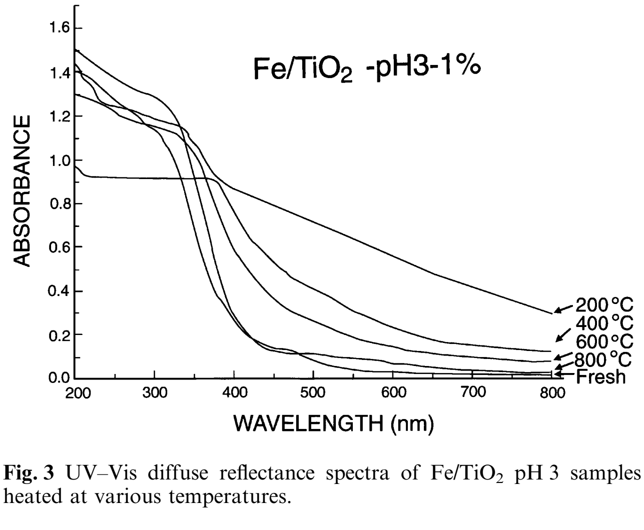

Fig. 3 UV–Vis diffuse reflectance spectra of Fe/TiO_2 pH 3 samples heated at various temperatures.

Table 2 Mössbauer characterization of Fe/TiO_2 (1% wt) samples

Sample	Sub-spectrum	Δ/mm s^{-1}	δ/mm s^{-1}	Hyperfine field	Abundance (%)	Species
Fe/TiO_2 pH 3 70 °C	Doublet	0.5916	0.4562	—	100	Fe^{3+}
Fe/TiO_2 pH 3 200 °C	Doublet	0.8321	0.4299	—	100	Fe^{3+}
Fe/TiO_2 pH 3 400 °C	Doublet	0.6063	0.4594	—	100	Fe^{3+}
Fe/TiO_2 pH 3 600 °C	Doublet	0.7585	0.4200	—	33.19	Fe^{3+}
	Sextet	−0.349	0.389	52.61	66.81	Fe^{2+} Hematite
Fe/TiO_2 pH 3 800 °C	Doublet	0.5920	0.4231	—	50.67	Fe^{3+}
	Sextet	−0.1538	0.3648	52.48	49.33	Fe^{3+} Hematite

obtained are reported in Table 1. Thermal treatment of the samples is seen to modify the band gap with increasing temperature leading to an increase in E_g. Band gap values of 3.0 eV for the sample treated at 800 °C and 2.2 eV for the sample treated at 200 °C are reported in Table 1 while values of 2.6 and 2.4 were obtained for the samples treated at 400 and 600 °C, respectively. The modification of E_g upon thermal treatment is likely due to the structural rearrangement of titania. When a number of titania phases co-exist E_g seems to be reduced.

Mössbauer spectroscopy

Mössbauer spectra are shown in Fig. 4. The Mössbauer parameters, the isomeric shift δ and the quadrupolar splitting Δ, are both given in mm s^{-1} using ^{57}Co embedded in metallic iron as the gamma photon source. Although the samples were prepared with $FeCl_2$ in hydrochloric acid complete oxidition to Fe^{3+} was observed under the conditions used. However the effect of thermal treatment leads to dehydroxylation or residual desorption of highly reducing OH^- and reduction of a portion of Fe^{3+} is thus possible in samples treated at 600 and 800 °C. Table 2 indicates the co-existence of Fe^{2+} and Fe^{3+} in such samples.

Below 400 °C (Fig. 4(c), (d) and (e)), both the isomeric shift δ and quadrupolar splitting Δ, remain almost constant (Table 2). When the thermal treatment temperature is increased to 600 and 800 °C, doublet and sextet spectra (Fig. 4(a) and (b)) are observed and the δ and Δ values clearly decrease. This is a characteristic behavior of the co-existence of Fe^{3+} and Fe^{2+} in natural clays but has not been reported previously in Fe/TiO_2 solid mixtures.

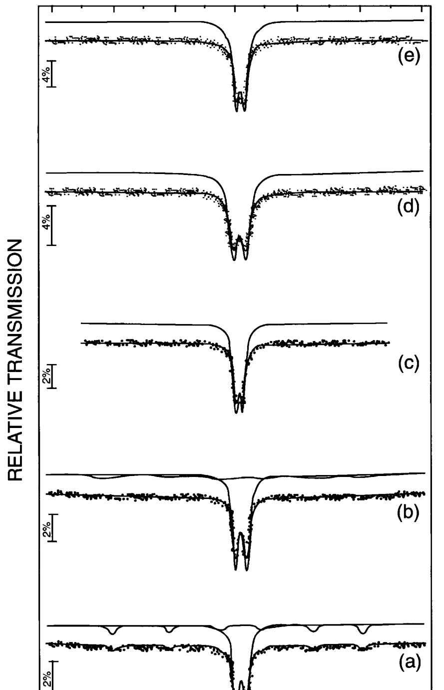

Fig. 4 Mössbauer spectra of Fe/TiO_2 pH 3 samples treated at various temperatures: (a) 800 °C, (b) 600 °C, (c) 400 °C, (d) 200 °C and (e) 70 °C.

Conclusions

Materials containing Fe^{2+} and Fe^{3+} ions in TiO_2 matrices have been successfully prepared using $FeCl_2$ as iron precursor.

X-Ray diffraction patterns of samples heated at 70, 200 and 400 °C show the co-existance of brookite, anatase and rutile TiO_2 phases, the major phase being anatase. In samples treated at 600 °C the brookite phase disappears and rutile becomes the main phase. At 800 °C only the rutile phase is observed.

As the temperature is raised, the UV–Vis spectra show that the forbidden band gap, E_g, increases. The highest E_g value was obtained in the titania showing the rutile phase. In titania where brookite, anatase and rutile phases coexist the E_g is lowest.

Mössbauer characterization show that Fe^{2+} and Fe^{3+} coexist in the structure of titania treated at high temperature. A reducing effect of residual OH desorbed for high temperature calcined samples is proposed.

Acknowledgement

We acknowledge CONACYT for the support given to this work.

References

1 T. López, E. Sánchez, P. Bosch, Y. Meas and R. Gómez, *Mater. Chem. Phys.*, 1992, **32**, 141.
2 G. Pecci, P. Reyes, T. Lopez and R. Gomez, *Appl. Catal. A*, 1998, **17**, L7.
3 J. L. Boldú, E. Muñoz, X. Bokhimi, O. Novaro, T. López and R. Gómez, *Langmuir*, 1999, **15**, 32.
4 T. Lopez, R. Gomez, G. Pecci, P. Reyes, X. Bokhmi and O. Novaro, *Mater. Lett.*, 1999, **40**, 59.
5 T. Lopez, O. Chimal, M. Asomoza, R. Gomez, X. Bokhimi, O. Novaro and R. D. Gonzalez, *J. Solid State Chem.*, 1999, **144**, 349.
6 G. Pecchi, P. Reyes, F. Orellana, T. Lopez, R. Gomez and J. L. G. Fierro, *J. Tech. Biotech.*, 1999, **74**, 1.
7 T. Lopez, J. Hernandez, R. Gomez, X. Bokhimi, J. L. Boldu, E. Muñoz, O. Novaro and A. Garcia-Ruiz, *Langmuir*, 1999, **15**, 5689.
8 T. Lopez, J. Hernández-Ventura, M. Asomoza, A. Campero and R. Gómez, *Mater. Lett.*, 1999, **41**, 399.
9 P. Kumar Krishnankutty-Nair, *Appl. Catal. A.*, 1994, **119**, 163.
10 X.-Z. Ding, X.-H. Lui and Y.-Z. He, *J. Mater. Sci. Lett.*, 1996, **15**, 1789.
11 H. Kominami, Y. Takada, H. Yamagiwa, Y. Kera, M. Inoue and T. Inui, *J. Mater. Sci. Lett.*, 1996, **15**, 197.
12 X. Bokhimi, J. L. Boldú, E. Muñoz, O. Novaro, T. Lopez, J. Hernández-Ventura, R. Gómez and A. García-Ruiz, *Chem. Mater.*, 1999, **11**, 2716.

13 M. G. Keith and J. R. Chelikowsky, *Am. Phys. Soc.*, 1992, **46**, 3.

14 W. F. Smith, *Science and Engineering Materials Foundations*, McGraw-Hill, México City, 3rd edn., 1993.

15 A. Cox and T. J. Kemp, *Introductory Photochemistry*, McGraw-Hill, México City, 2nd edn., 1971.

16 A. Hernández, L. M. Torres-Martinez and T. Lopez, *Mater. Lett.*, 2000, **45**, 340.

17 E. Muñoz, J. L. Boldu, E. Andrade, O. Novaro, T. Lopez and R. Gomez, *J. Am. Ceram. Soc.*, 2001, **84**, 392.

18 U. Selvaraj, A. V. Prasadarao, S. Komarneni and R. Roy, *J. Am. Ceram. Soc.*, 1992, **75**, 1167.

19 B. E. Yoldas, *J. Mater. Sci.*, 1986, **21**, 1087.

20 R. J. H. Clark, *The Chemistry of Titanium and Vanadium*, Elsevier, New York, 1968, ch. 9.

21 H. Al-Ekabi and N. Serpone, *J. Phys. Chem.*, 1988, **92**, 5726.

22 H. Chih-Wen, A. S. T. Chiang, L. Cheng-Chung and Y. Sheng-Jenn, *J. Non-Cryst Solids*, 1992, **144**, 53.

23 J. L. Sohn and H. J. Jang, *J. Mol. Catal.*, 1991, **64**, 349.

24 A. F. Cotton and G. Wilkinson, *Advanced Inorganic Chemistry*, J. Wiley, New York, 3rd edn., 1972.

25 G. W. Brady, M. B. Robin and J. Varimbi, *Inorg. Chem.*, 1964, **3**, 1168.

26 E. López-Salinas, J. G. Hernandez-Cortez, M. A. Cortes-Jacome, J. Navarrete, M. E. Llanos, A. Vazquez, H. Armendariz and T. Lopez, *Appl. Catal.*, 1999, **127**, 43.

27 K. Nakamoto, *Infrared and Raman Spectra of Inorganic and Coordination Compounds*, John Wiley & Sons, New York, 1992, p. 335.

28 F. Boccuzzi, S. Coluccia, G. Ghiotti, C. Monterra and A. Zecchina, *J. Phys. Chem.*, 1978, **82**, 1298.

29 Y. Zhao, X. P. Xu, J. M. Gao and Y. Tang, *J. Raman Spectrosc.*, 1996, **27**, 549.